물리탐사
Vol. 4, No. 4, 2001, p. 133~144

High-Resolution Seismic Reflection Profiling on Land with Hydrophones Employed in the Stream-Water Driven Trench

Ji-Soo Kim[1], Su-Hyung Han[1], Hak-Soo Kim[2], Won-Suk Choi[2] and Chang-Ho Jung[2]

하천수유입과 하이드로폰을 이용한 육상 고분해능 탄성파반사법탐사

김지수[1] · 한수형[1] · 김학수[2] · 최원석[2] · 정창호[2]

Abstract : An effective seismic reflection technique for mapping the cavities and bedrock surface in carbonate rocks is described. The high resolution seismic reflection images were successfully registered by using the hydrophones employed in the stream-water driven trench, and were effectively focused by applying optimal data processing sequences. The strategy included enhancement of the signal interfered with the large-amplitude scattering noise, through pre- and post-stack processing such as time-variant filtering, bad-trace editing, residual statics, velocity analysis, and careful muting after NMO (normal moveout) correction. The major reflections including the bedrock surface were mapped with the desired resolution and were correlated to the seismic crosshole tomographic data. Shallow major reflectors could be identified and analyzed on the AGC (auto gain control)-applied field records. Three subhorizontal layers were identified with their distinct velocities; overburden (<3000 m/s), sediments (3000-4000 m/s), limestone bedrock (>4000 m/s). Taking into account of no diffraction effects in the field records, gravel-rich overburdens and sediments are considered to be well sorted. Based on the images mapped consistently on the whole survey line and seismic velocity increasing with depth, this area probably lacks in sizable cavities (if any, no air-filled cavities).

주요어 : 고분해능 탄성파반사법, 하이드로폰, 트렌치, 자료처리

요 약 : 석회암지역에서 공동 및 기반암 표면을 파악하기 위한 효율적인 탄성파반사법탐사의 자료수집과 처리기법을 연구하였다. 트렌치 굴착 후 하천수유입과 하이드로폰을 이용하여 고분해능 탄성파반사자료를 성공적으로 얻을 수 있었고 효율적인 자료처리기법을 통하여 주요 반사면을 재건할 수 있었다. 자료처리는 중합전후에 걸쳐서 시변필터, 불량트레이스 제거, 잔여정보정, 속도분석, NMO보정 후 뮤팅 작업 등으로 고진폭 잡음에 가려있는 미약한 반사 이벤트를 강화시키는데 초점을 두었다. 만족할만한 분해능으로 규명된 기반암표면을 포함한 주요 반사면들은 탄성파 공대공 토모그래피 자료와 잘 상관되었으며 또한 AGC만이 적용된 현장자료에서 그 반사에너지를 확인할 수 있었다. 지하구조는 속도분포를 고려하여 크게 표토층(3000 m/s 이하), 퇴적층(3000-4000 m/s), 기반암(4000 m/s 이상)의 3개 층으로 구분할 수 있는데 자갈이 많이 분포하는 표토층 및 퇴적층은 현장자료에서 회절효과가 뚜렷이 나타나지 않은 점으로 미루어 분급 상태가 양호한 것으로 보인다. 또한 기반암표면 반사에너지가 전체 측선에 걸쳐 일관되게 나타나고 속도가 깊이에 따라 계속하여 증가하는 점으로 보아 공동(적어도 공기로 충진된 공동)은 분포하지 않은 것으로 해석된다.

Keywords : high-resolution seismic-reflection method, hydrophone, trench, data processing.

Introduction

Seismic reflection surveying is the most widely used geophysical technique, and has been since the 1930s. Its predominant applications are hydrocarbon exploration and research into crustal structure, with depths of penetration of many kilometers now being achieved routinely. Since around 1980s, the method has been applied increasingly to engineering and environmental investigations where depths of penetration are typically less than 200 m (Steeples and Miller, 1990; Miller and Steeples, 1991; Reynolds, 1997, Miller *et al.*, 1995). Advances have been made in the past decade in seismic reflection techniques, both in data acquisition and in data processing, to image subsurface structures at shallow depth.

Reflection seismic imaging of shallow events is often

*2001년 7월 24일 접수
1) 충북대학교 지구환경과학과(Dept. of Earth and Environmental Sciences, Chungbuk National University, Chongju 361-763, Korea)
2) 지오제니 컨설턴트(GeoGeny Consultants Group Inc., BangbaeDong, SeochoGu, Seoul 137-060, Korea)

more difficult than the deep crustal sounding both in detection capability and resolution, because reflection events caused by near-surface discontinuities are much more irregular and discontinuous. This often results in low S/N (signal-to-noise ratio) data, distortion of signals, and contamination by various near-surface noises (Mair and Green, 1981; Brown *et al.*, 1989; Kim *et al.*, 1994).

This research is aimed at mapping the limestone cavities (if they exist) and investigating the stability of the bridge and ultimately providing relevant inputs towards designing the reinforcement work for the road expansion. Geologically three study area, located on the roadway 38 in the vicinity of MiroMyon of SamchukGun, KangwonDo, belongs to the Late Paleozoic Limestone Group (KGS, 1998).

The overburden is abundant in gravels, which may produce poor S/N energy due to diffraction and poor geophone-coupling. Taking into consideration of very shallow groundwater level, we excavated trenches down to 1-2 m depth, to which stream-water was driven (Fig. 1). This process saturates the subsurface materials, and therefore, hydrophones can be an effective receiver for registering the higher frequency components in such an environment (Reynolds, 1997).

The data sets were processed in this study to image the very shallow reflectors in the depths up to 10m by focusing on complete removal of possible noise (surface wave, scattering noise, refraction, bad traces and NMO-stretched data) at shallow depth to allow more effective processing steps such as computation of stack power, residual statics and velocity analysis. The main purpose of this experiment was to delineate the shallow reflectors within carbonate rocks rather than to investigate geological boundaries.

Therefore, the pre-stack processing focused on preserving the frequency contents and amplitude rather than improving the vertical resolution with spectral balance or deconvolution, which may introduce undesirable artifacts and distortion from the high noise content in the data itself. Further, because the data set was thought to be characterized by a low S/N, the processing was focused on increasing S/N of the data by attenuating various types of noise, shot and/or receiver statics before stack and improving the resolution and lateral continuity after stack.

Prior to estimating the correlation between the seismic data and the geological section, a segment of the highly reflection zone was investigated on the AGC-applied field records and correlated to available seismic tomogram from a test borehole. This correlation would comprise the basic information for the data processing.

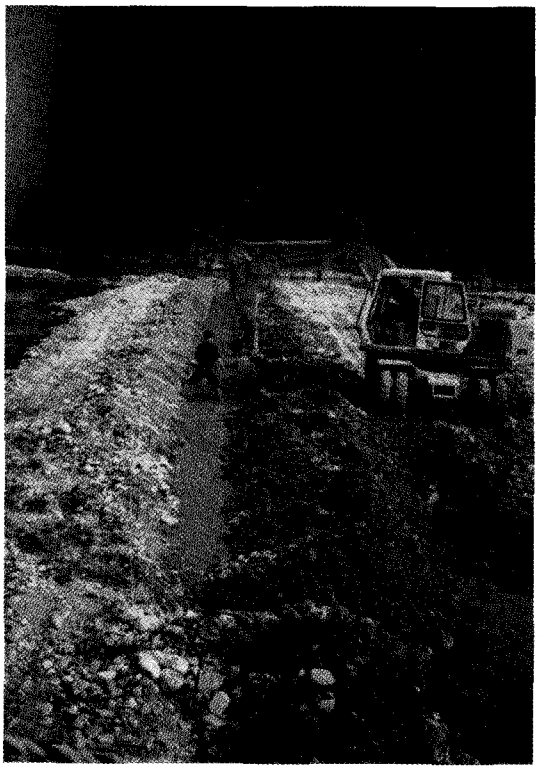

Fig. 1. Stream-water driven in the trench.

Data Acquisition

There are four short reflection profiles; MR1, MR2, MR3, and MP1 (Fig. 2). Line MP1 is located approximately 1 km north from the line MR1. Table 1 lists the acquisition parameters used in the field. The groundwater level was reported to be only 2 m deep. Consequently, it was decided that the seismic source attempted to be fired into fully water-saturated sediments, which is ideal for high resolution seismic reflection profiling. Therefore, it was designed mainly to map shallow and thin reflectors in the carbonate rocks, with fairly close receiver spacing and fine sampling rate.

The spread of 48 hydrophones was placed along each trench with an interval of 1 m. The spread type employed in this study is variant depending on the field condition. As an example, the line MR1 comprises the split-spread for the eastern segment and end-on spread for central and western segments of the survey line (Fig. 3). Therefore, the line MR1 is 71m long in total, with corresponding subsurface coverage of 63 m.

The energy source used was electrical detonators; combi-

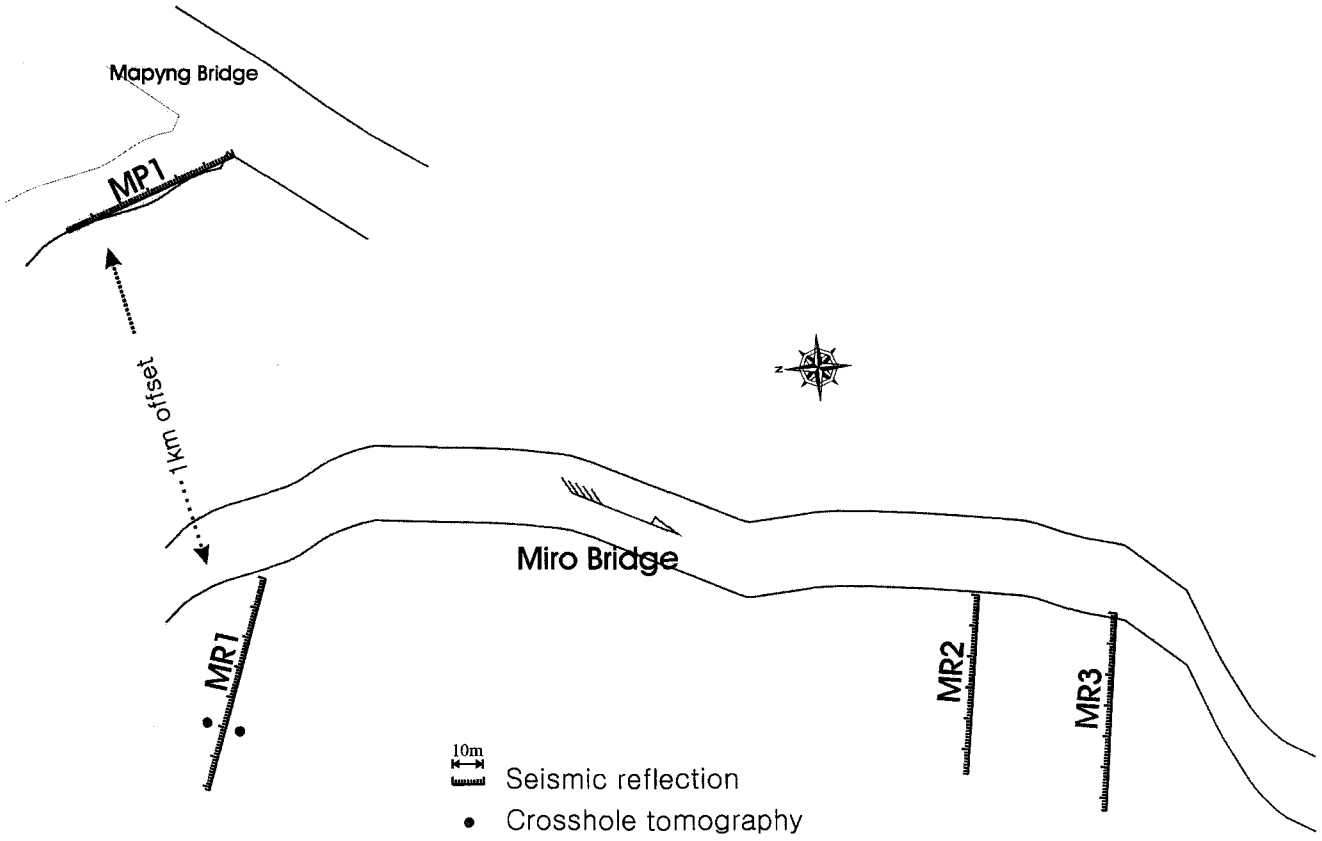

Fig. 2. Seismic reflection lines MR1, MR2, MR3, and MP1 on the MiroMyun of SamchukGun, KangwonDo. The line MP1 is located approximately 1 km north from the line MR1.

Table 1. Field acquisition parameters

Parameters	Remarks
source type	special detonator(1g) + general detonator(3g)
receiver type	hydrophone
spread type	end-on, split-spread
number of channels	48
shot interval	2 m
receiver interval	1 m
receiver depth	about 1 m
coverage	2400%
sampling rate	1/16 ms
record length	128 ms

nation of general detonator (3 g) for powerful energy and special detonator (1 g) designed at Hanhwa Energy Ltd. for minimum-delay detonation (less than 0.002 ms) (Kim *et al.*, 2000a).

The seismic recording instrument used was 48-channel DMT Compact/Summit with a 32 bit A/D converter, which recorded 128 ms length, providing theoretically 225 m of depth of penetration (based on the velocity of 3500 m/s), with sampling interval of 1/16 ms.

Data Processing

The data were processed at the Chungbuk National University using the VISTA processing software package and programs developed in-house. Prior to processing, the raw SEG-2 format data were reformatted into the standard SEG-Y format. The problems with the field record were expected from the presence of strong shot-generated surface waves, low S/N, and traveltime distortion caused by near-surface irregularities such as gravel surfaces. All of these limitations affect the shallow depth experiments.

The basic strategy to image the shallow fracture zones with the desired resolution included: editing of bad traces (depending on the early observable arrivals), time-variant filtering on shot gather, residual statics on NMO corrected receiver and/or shot gathers before stack, and f-k filtering after stack. Figure 4 shows a detailed flowchart for data processing (Kim *et al.*, 2000b).

Based on the information learned from the spectral analysis (Fig. 5a, b, c) for the raw data with only AGC applied (Fig. 6a), the dominant frequency of the data is around

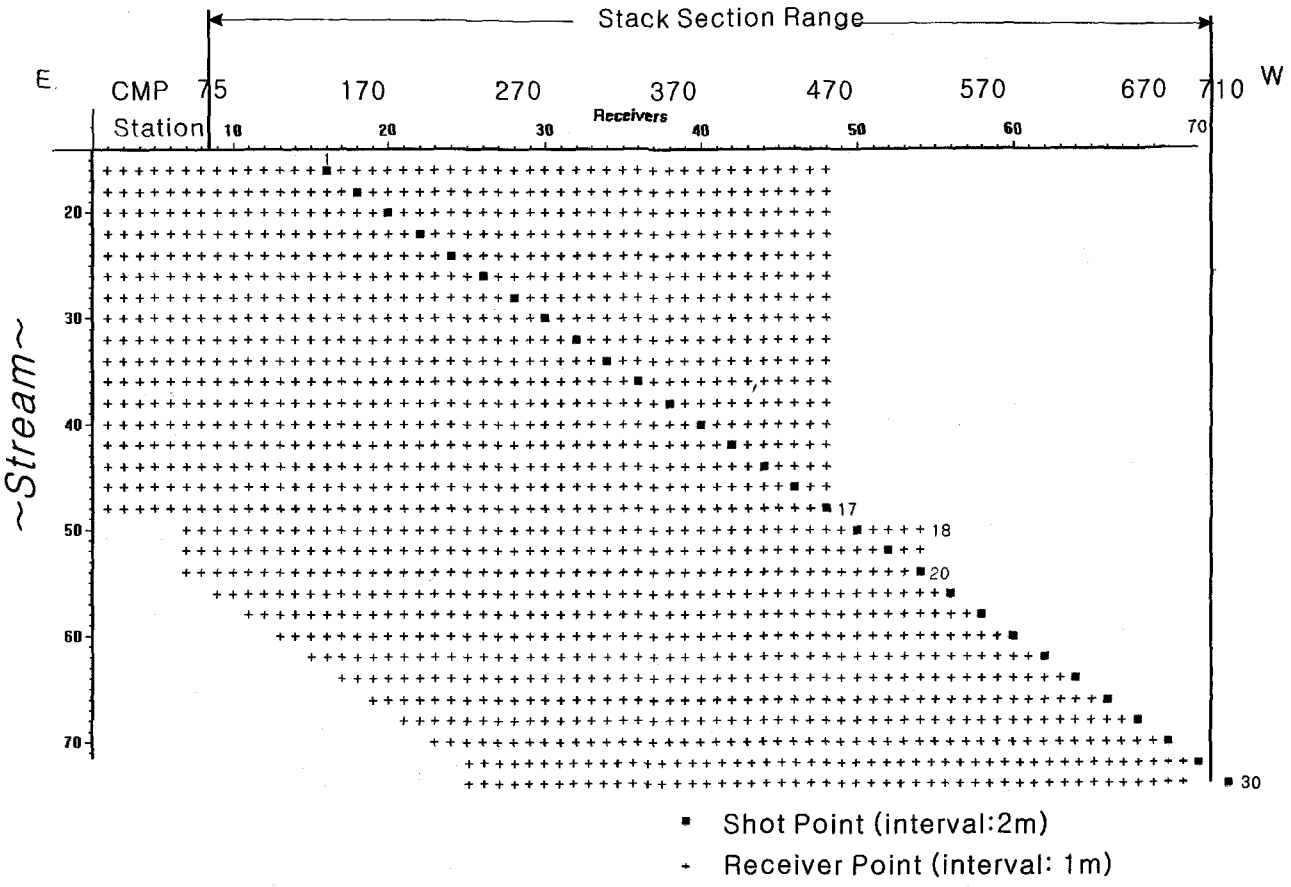

Fig. 3. Location of shot points, receiver points, and common mid-points (CMP) for the line MR1.

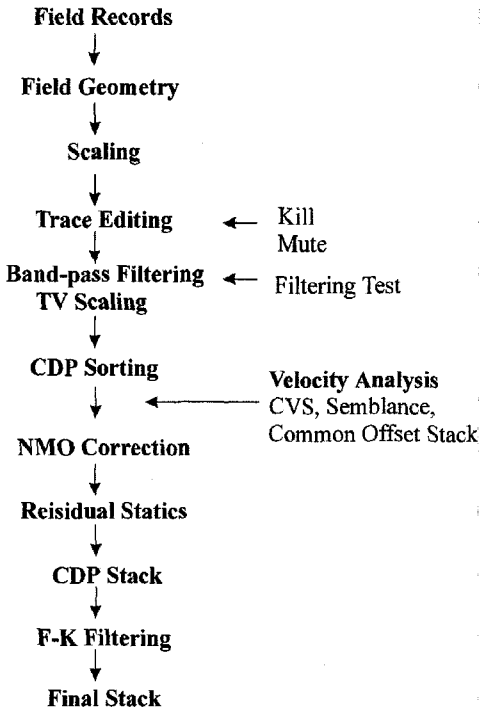

Fig. 4. Processing flowchart used for data processing.

800 Hz but the signal is spread up to 2000 Hz (Fig. 5a, b). The higher frequency (>2000 Hz) with cyclic ringing is probably associated with electrical noise due to detonation (Fig. 5c). The application windows for the Figures 5a, b, c are represented by a full trace, RE (reflection), and NO (noise) in the Figure 6a, respectively. To focus on the relatively shallow reflector by faithfully preserving high-frequency component. bandpass filter with pass band 50-100-800-1000 Hz was applied to all traces (Fig. 6b). Strong ground roll and scattered energy observed in Figure 6a could be effectively attenuated with bandpass filtering, but the ringing (i.e., electrical noise) was simultaneously boosted. Such a very high-frequency noise was effectively reduced by time-variant filtering of the raw data (Fig. 6c). Each reflection event at 20 ms and 30 ms is more clearly identified as a typical hyperbola.

The field statics were found to be quite small. Maximum time shifts for field statics were in the range of 1-3 ms. Receiver-hole depth corrections were performed with respect to a depth of 1m to compensate for the variation of the hole

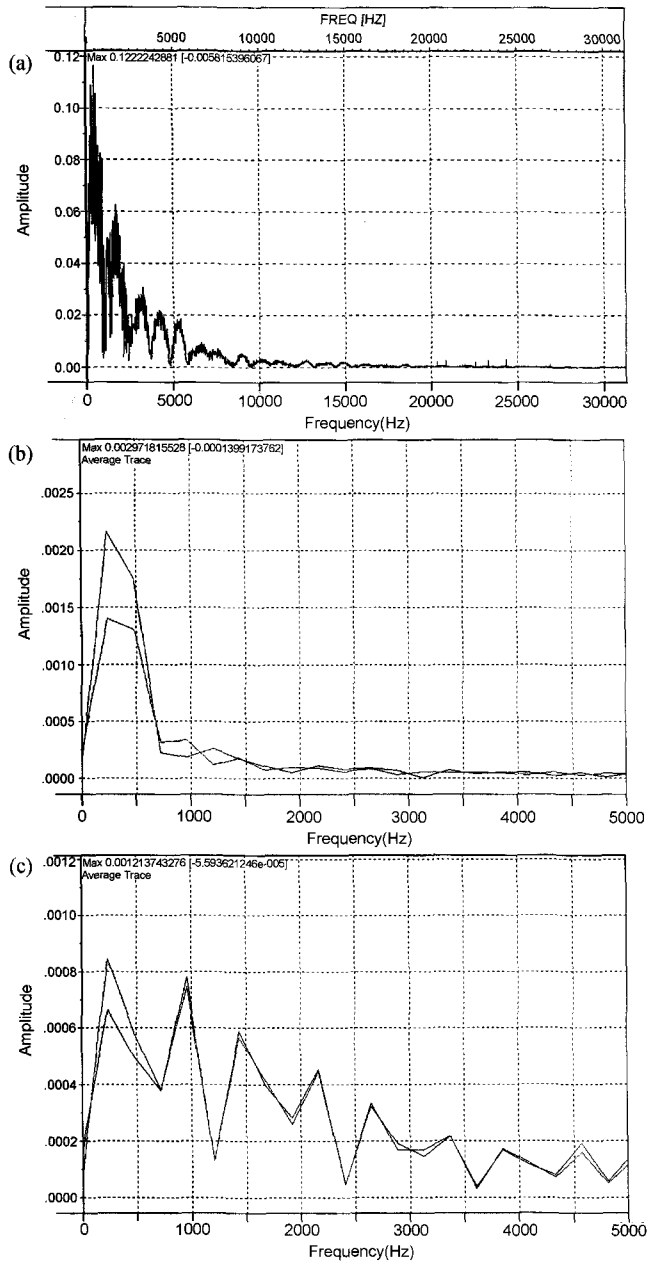

Fig. 5. Amplitude spectrum of (a) a trace, (b) signal portion, and (c) electrical noise. The application windows for (a), (b), and (c) are represented by a trace, reflection (RE), and noise (NO) of the Figure 6, respectively.

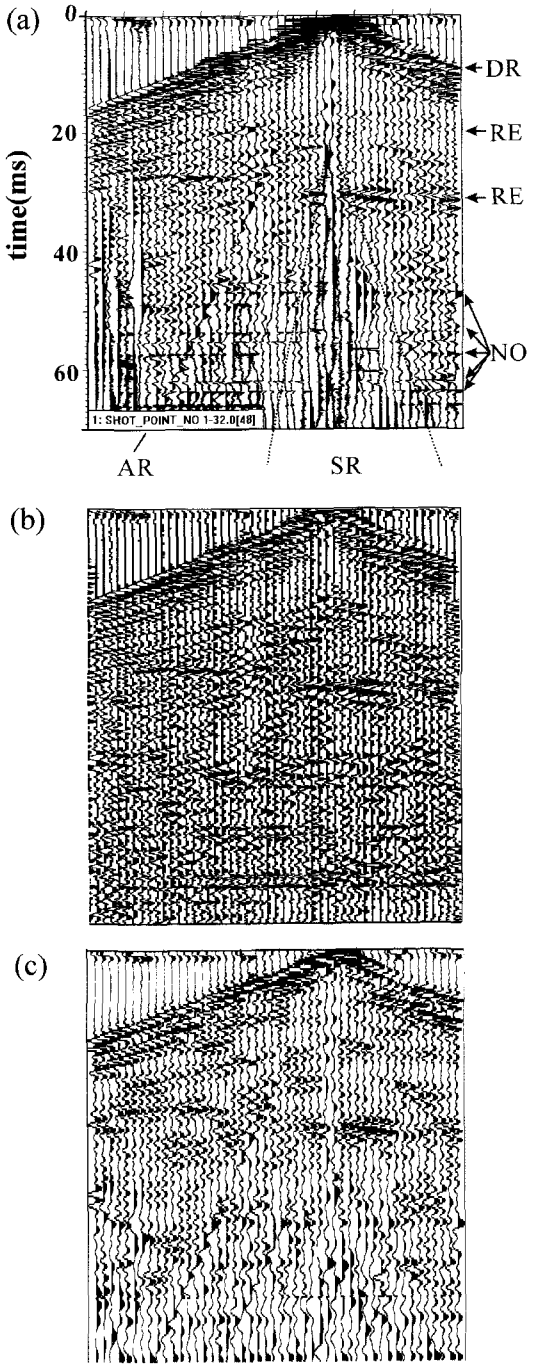

Fig. 6. Line MR1 shot gather: (a) raw data; (b) bandpass filtered data with passband 50-100-800-1000 Hz; and (c) time-variant filtered data with Ormsby frequency band ranging from 50-2000 Hz to 50-60 Hz. The input is the raw data. (DR: direct wave, RE: reflection, NO: electric noise, AR: air wave, SR: surface wave)

depth before residual statics correction was applied. Residual statics correction is critical in imaging shallow reflectors (Milkereit *et al.*, 1991; Kim *et al.*, 1994) since it compensates for near-surface irregularities. The stack power maximization method (Ronen and Claerbout, 1985), known to be effective for poor S/N data and low-fold data, were tested and applied to these data sets. Super traces were formed from a small number of gathers (4 NMO corrected CMP (common mid-point) gathers) to limit structural influence. To prevent cycle skips, the maximum allowable shift was chosen as small as 2 ms.

The improved resolution through various focusing steps are clearly shown in NMO corrected CMP gather (Fig. 7) and stack section (Fig. 8). The significant improvement in

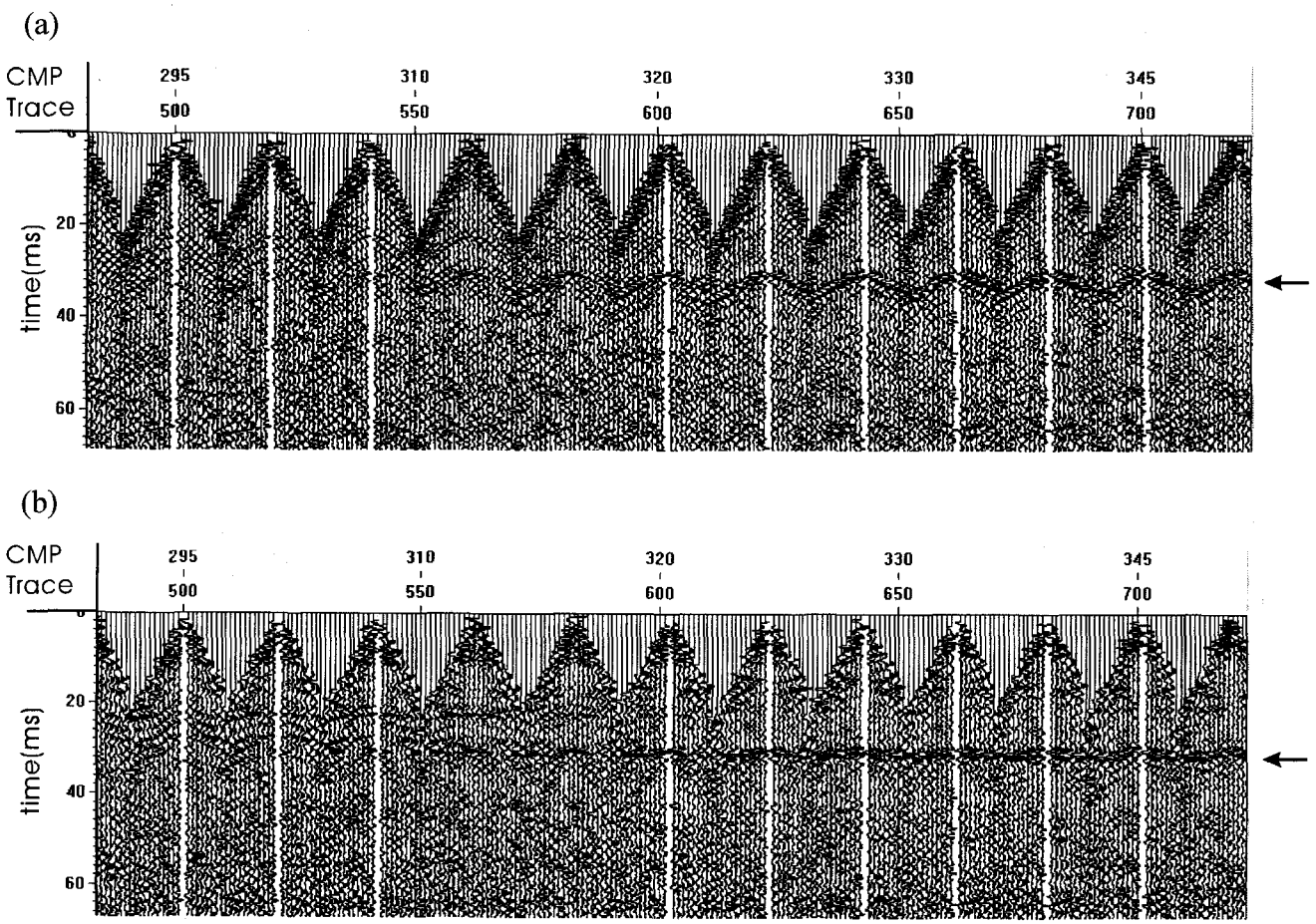

Fig. 7. Sample CMP gathers from line MR1: (a) AGC-applied and (b) NMO-corrected. The arrow represents the reflection from the bedrock surface.

the strength and continuity of the event is evidenced by two reflections indicated by arrows in Figure 8. The second and bottom layers are interpreted to be sediments and limestone bedrock, respectively.

The stack sections for the lines MR1, MR2, MR3, and MP1 (Figs. 9a, b, c, d) reveals well-focussed event in the time window 7 ms (about 5 m)-30 ms (about 33 m). The depths for the events were estimated on basis of RMS velocity (1400 ms/ at 7 ms; 2200 m/s at 30 ms) rather than interval velocity. Major events represented by the arrows appear to be mapped consistently on the whole survey line. These reflections are probably from the bedrock surface. The weakly reflective nature within the sediments for the lines MR1 (Fig. 9a) and MP1 (Fig. 9d) most likely originates from the interlayered lithological boundaries (i.e., between silty sand and gravel) or possibly the basal plane of the groundwater saturation. Further studies on the auxiliary data such as borehole and tomography data will be required to accurately investigate the splay of the sediments at the northern part of the area (i.e., lines MR1 and MP1)

Interpretation of Reflection Events

The shallow events at approximately 20 ms and 30 ms, considered to be reflections form the surfaces of sediments and bedrock, respectively, attempted to be investigated in field records and were correlated to the events in the seismic tomogram collected in the vicinity of the line MR1.

Investigations of Field Records

Analysis of the field data is an important strategy for investigation of seismic images of shallow reflection events, because field records comprise the basic data processing. Major reflection images are usually visible on shot gathers, although they are often contaminated with ground roll and misaligned due to other surface irregularities. For the analysis of the basic data, the field records were only scaled for amplitude restoration with AGC.

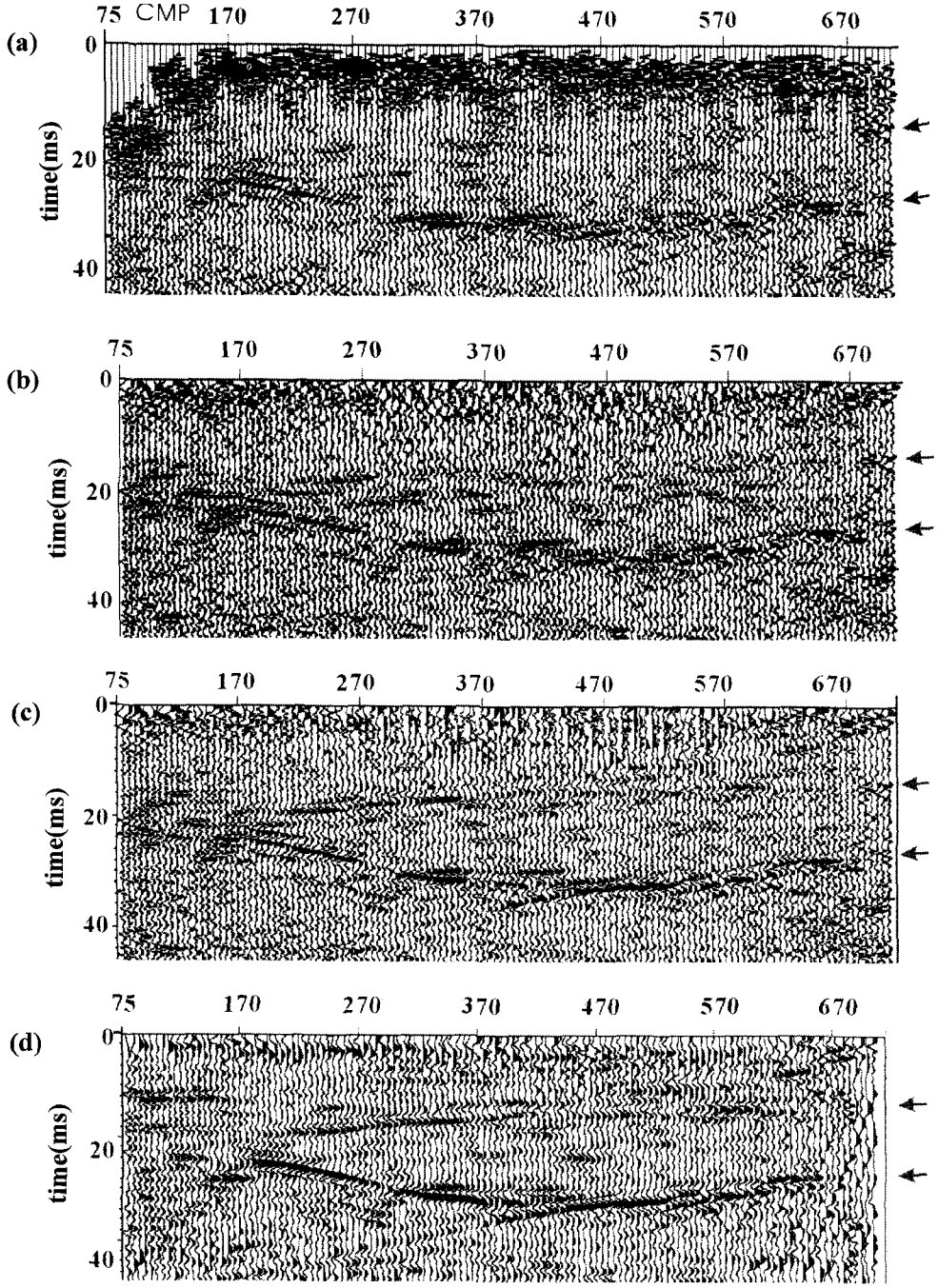

Fig. 8. Improved resolution with application of filtering and statics correction: (a) brute stack section; (b)section after time-variant filtering; (c) section after time-variant filter and residual statics, and (d) section after time-variant filter, residual statics, and post-stack f-k filtering. The upper and lower arrows represent the reflections from the top of the weathered rock and bedrock, respectively.

The rightward- and leftward-dipping trends of the major event (indicated by an arrow) (Fig. 10a) are also indicated in the AGC-applied field records (Fig. 10b) by strong reflection energy around the leftward-shifted (shot points 7, 8) and rightward-shifted (shot points 23, 24) axes of the reflection hyperbola, respectively. As the shot from the point (7, 8) moves toward central shot point (15, 16), the traveltime from the major reflector in the corresponding shot gathers increase to about 35 ms and apex is stationary at shot points because the interface becomes deeper and flattened at stations 15 and 16. Once the shot point approaches to the right side end-point, the travel time is slightly reduced. Such a trend is suggested by leftward dipping event, as shown in the stack section (Fig. 10a).

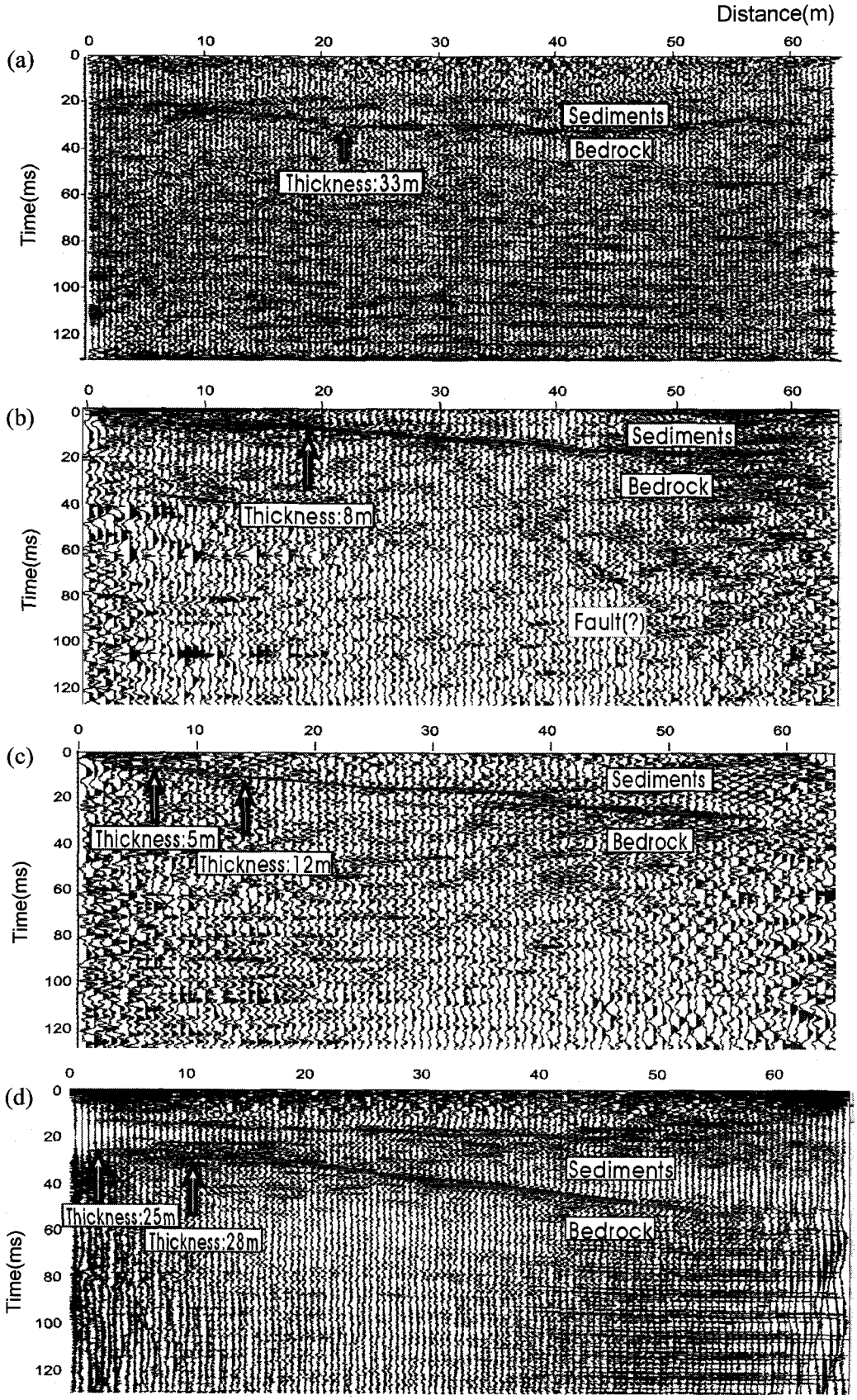

Fig. 9. Final stack section for the lines of (a) MR1, (b) MR2, (c) MR3, and (d) MP1. Splays of sediments are shown in the lines MR1 and MP1.

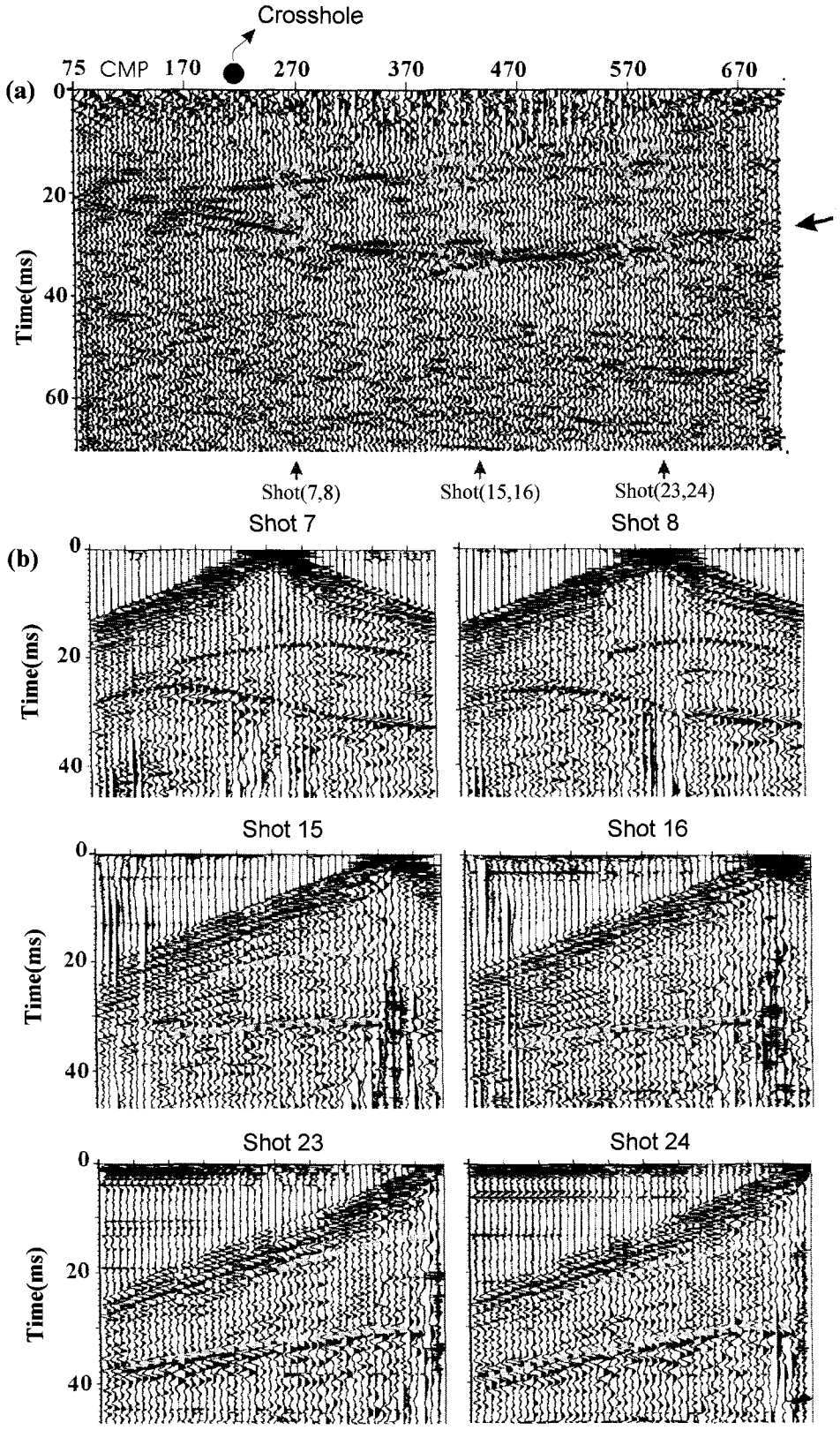

Fig. 10. Examination of reflection energy for the line MR1: (a) stack section, (b) a sample of shot records. Arrows represent the major reflection from bedrock surface.

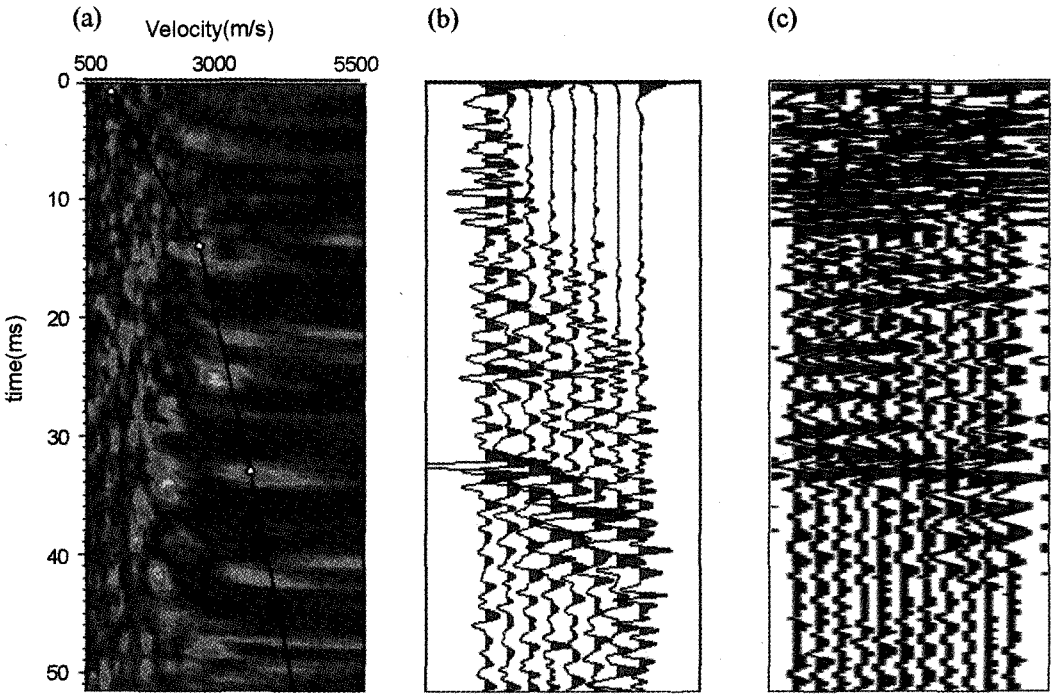

Fig. 11. Velocity spectrum analysis: (a) velocity semblance plot; (b) offset gather; (c) constant velocity scan. The velocity-time pairs are approximated as (10 ms, 2000 m/s), (20 ms, 3000 m/s), (30 ms, 4000 m/s).

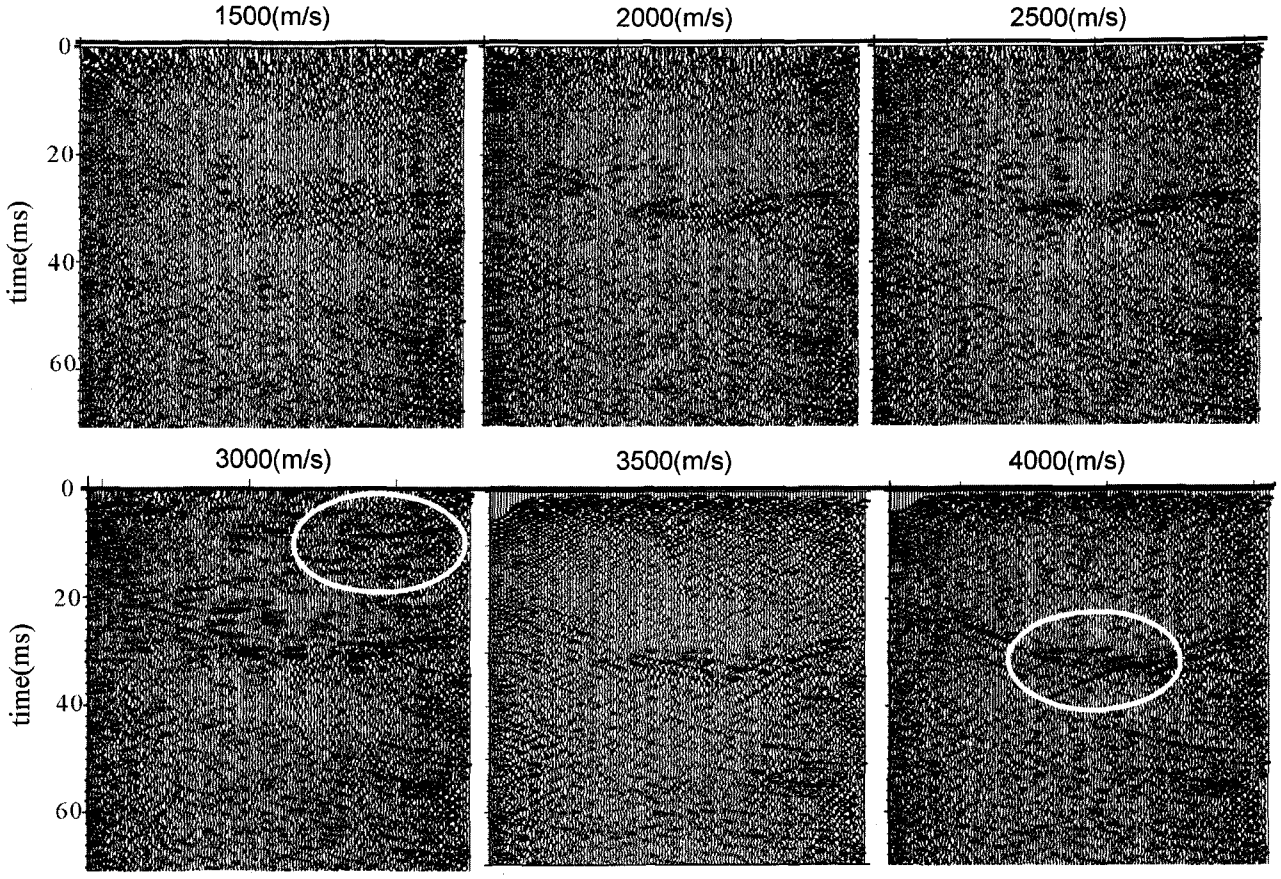

Fig. 12. Constant velocity stack. The upper and lower reflectors are best focused with velocity value of 3000 m/s and 4000 m/s, respectively.

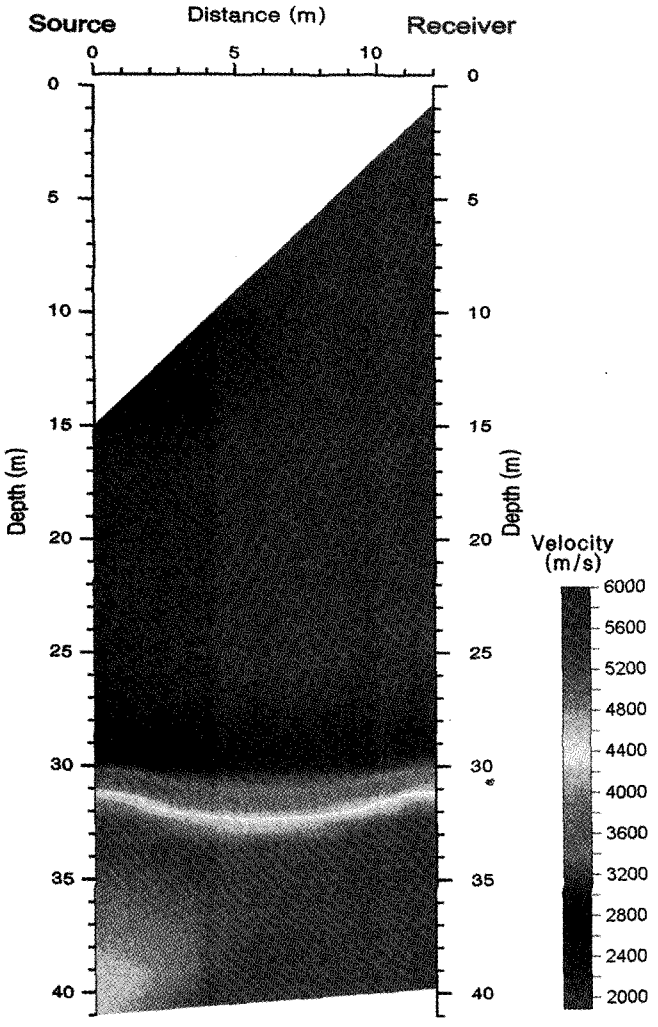

Fig. 13. Seismic tomogram. The round-shaped event at depth of approximately 32 m are believed to be bedrock surface, which is well correlated to the seismic reflection images (Fig. 9a).

Velocity Analysis

Seismic data processing requires estimation of accurate velocity profile as a function of depth. To determine the seismic velocity profile as a function of two-way traveltime, the velocity spectral analysis was performed (Fig. 11).

From the matrix of chosen coherency and velocity function versus time function, velocity-time pairs were picked for each coherency peak. The velocity-two way time pairs approximated from this velocity semblance approach are as follow: 0 ms: 900 m/s; 10 ms: 2000 m/s; 20 ms: 3000 m/s; 30 ms: 4000 m/s.

As an alternative, constant velocity stack (CVS) test was performed. Figure 12 shows a stack section which has been corrected repeatedly using a range of constant velocity values between 1500-4000 m/s. The two major reflectors, clearly identified in the stack section, are correlated to the events focused in the CVS panel tests.

The representative velocities estimated from the seismic reflection data are as follows: overburden (<3000 m/s), sediments (3000-4000 m/s), limestone bedrock (>4000 m/s). These values and the corresponding depths are also well correlated to the results from the crosshole seismic tomography which was earlier independently performed (Fig. 13) (Kim *et al.*, 2000a).

Conclusions

Application of seismic reflection techniques in geological engineering problems involve two specific phases; careful planning and acquisition of data in the field and data processing and imaging of the subsurface target features.

By using hydrophones in the stream-water driven trench and employing appropriate processing sequence and parameters, shallow reflectors in carbonate rock environment can be delineated and imaged with reasonable confidence using high-resolution reflection survey technique. In particular, the attenuation of ground roll, the exclusion of bad records, complete rejection of the NMO-stretched portion, time-variant filtering, and careful statics are critical processing steps for the low S/N data often typical of records from the carbonate rock environment.

The seismic reflection images of shallow fracture zones correlate well with the results from earlier seismic tomographic data. Careful investigation of preprocessed field records provide clues to identification of the bedrock surface and lithologic boundaries, and analysis of their trends.

On the basis of velocity information from the constant velocity stack, and tomographic images, there exist three subsurface layers: overburden (<3000 m/s), sediments (3000-4000 m/s), limestone bedrock (>4000 m/s). The gravel-rich overburden is considered to be well sorted because the reflection energy from the overburden appears to be aligned rather than diffracted. With respect to the existence of the cavities, there may be no sizable cavities because reflection images are consistently mapped on the whole survey line and seismic velocity increases with depth.

More carefully planned high resolution seismic surveys and the appropriate processing discussed here is readily applicable to engineering seismic reflection survey, especially for the water-saturated area.

Acknowledgements

This research was primarily supported by the Industry Technical Support Program 2000 of the Korea Science and Engineering Foundation operating grant to J.S. Kim. Authors thank Dr. H.Y. Lee (Korea Institute of Geology, Mining and Materials) and Prof. S.R. Shin (Korea Maritime University) for their constructive reviews.

References

Brown, A., Soonawala, N. M., Everitt, R. A., and Kamineni, D. C., 1989, Geology and geophysics of the Underground Research Laboratory site, Lac Du Bonnet Batholith, Manitoba: *Can. J. Earth Sci.*, **26**, 404-425.

KGS (Korean Geological Society), 1998, Geology of Korea: *Sigma Press*, Seoul, p. 802.

Kim, H. S, Choi, W. S., and Chung, C. H., 2000a, Geological and geophysical surveys for the expansion of the Miro-Samchuk Roadway: *Technical Report* (**12**), GeoGeny Consultant Inc. Seoul, 252p.

Kim, J. S., Moon, W. M., Lodha, G., and Soonawala, N., 1994, Imaging of reflection seismic energy for mapping shallow fracture zones in crystalline rocks: *Geophysics*, **59**, 753-765.

Kim, J. S., Han, S. H., Kim, H. S., and Choi. W. S., 2000b, Imaging of limestone-bedrock surface using high-resolution seismic reflection method: 4th Annual Conference of Korean Geophysical Society, Seoul, 30-31. (Abstract in Korean)

Mair, J. A., and Green, A. G., 1981, High resolution seismic reflection profiles reveal fracture zones within a homogeneous granite batholith: *Nature*, **294**, 439-442.

Miller, R. D., and Steeples, D. W., 1991, Detecting voids in a 0.6 m coal seam, 7 m deep, using seismic reflection: *Geoexplor.*, **28**, 109-119.

Miller, R. D., Anderson, N. L., Feldman, H. R., and Fransen, E. K., 1995, Vertical resolution of a seismic survey in stratigraphic sequences less than 100 m deep in southeastern Kansas: *Geophysics*, **60**, 423-430.

Milkereit, B., Percival, J. A., White, D., Green, A. G., and Salisbury, M. H., 1991, Seismic reflectors in high-grade metamorphic rocks, of the Kapuskasing uplift: *Am. Geophys. Union, Geodyn. Ser.*, **22**, 39-45.

Reynolds, J. M., 1997, An introduction to applied and environmental geophysics: *John Wiley and Sons*, New York, p. 789.

Ronen, J., and Claerbout, J. F., 1985, Surface-consistent residual statics estimation by stack-power maximization: *Geophysics*, **50**, 2759-2767.

Steeples, D. W., and Miller, R. D., 1994, Pitfalls in shallow seismic reflection: *Proceedings SAGEEP'94*, Englewood.